Int. J. Solids Structures, 1977, Vol. 13, pp. 683–697. Pergamon Press. Printed in Great Britain

A NEW HIGH-PRECISION STRESS FINITE ELEMENT FOR ANALYSIS OF SHELL STRUCTURES

M. GELLERT and M. E. LAURSEN
Structural Research Laboratory, Technical University of Denmark, Lyngby, Denmark

(*Received* 2 *September* 1976; *revised* 20 *December* 1976)

Abstract—A new high-precision finite element for analysis of shell structures is presented. It is derived from a slightly generalized equilibrium principle. Accordingly both stresses and displacements are obtained as primary result of analysis. At the assembly level the element has 45 degrees of freedom, all of them generalized displacements. For the price of some additional computational effort on the elemental level of analysis the proposed element is believed to gain certain advantages over the recently developed high-precision displacement elements. Thin as well as thick shell structures of arbitrary shape and loading can be equally analyzed. Engineering accuracy is attained with only very few elements. A variety of numerical examples demonstrates the applicability of the new element to all kinds of situations occuring in practice. A review of the existing high-precision shell elements is also included.

INTRODUCTION

The history of shell analysis by means of finite elements goes back to the early sixties. The first attempts of flat plate approximation have had only limited success due to the disregard of curvature coupling within each element. As a consequence a very large number of elements had to be used in order to achieve satisfactory accuracy. Inclusion of the curvature effect inside the element led to development of a variety of shallow shell approximations. Considerable improvements have been reported with these elements in comparison with the previous approach. However, in cases of deep shells with short wave length in displacement and/or stress distribution the shallow shell elements did not prove to be the radical answer for an efficient shell analysis. Indeed, any improvements made in representation of the shell variables and/or geometry ought to be ineffective if the governing differential equations and boundary conditions are not regarded with adequate rigour. It is doubtless that the recent development of many types of high precision shell elements has been largely influenced by the above mentioned argumentation. An exhaustive number of these are described in Refs. [1–10]. In Refs. [1–4] sophisticated triangular thin shell elements are presented. They are shown to be highly efficient (see also [11, 12]) in cases with smooth strain distribution. Unfortunately they are much less suitable when this is not the case as often occurs in situations with jumps in thickness or shell panel intersections. Very similar conclusions can be drawn for the various curved quadrilateral shell elements presented in [5–8] perhaps with exception of one of the versions in [5]. In that version a nonconforming element is obtained with only displacement and rotational degrees of freedom at nodes. A very attractive idea for a mixed-type shell element has been presented by Visser [9]. Relatively high order representation of the variables becomes possible with only 24 degrees of freedom per element. Furthermore shell intersection analysis is exhibited. Its drawback becomes evident when more than two panels intersect or a common boundary is subject to action of a prescribed normal moment distribution. In those cases a normal moment equilibrium equation must be added and the moments pertaining to the different elements should be kept as independent degrees of freedom. Another promising approach is that of Zienkiewicz *et al.* [10]. A quadrilateral shell element is derived from a three-dimensional isoparametric form by prescription of linear displacement variation across the thickness and supression of energy due to strain normal to the middle plane. Reduced numerical integration allows the element to be used in thick as well as in thin shell analysis. The five degrees of freedom at each node consist of purely displacement and rotation components. Accordingly "parabolic" 40 degree-of-freedom and "cubic" 60 degree-of-freedom elements are developed. Forces can be reproduced respectively up to first and second order accuracy provided the reduced numerical quadrature does not harm the moment accuracy. In Ref. [8] the whole approach is somewhat doubted on the basis of uncertainty of invariance and reciprocity satisfaction. This is further strengthened in Ref. [4] showing convergence of the isoparametric element to a shallow shell theory result. Numerical examples of a number of classical deep thin

shell problems would give a decisive engineering answer for the range of applicability of these elements.

This paper deals with a new curved triangular equilibrium shell element. The equilibrium finite element method was introduced by Fraeijs de Veubeke[13]. Though accuracy in stresses is in most cases of higher importance for the engineer than that of displacements, the method has not gained the expected popularity. In its earlier form it was less suitable for creation of a general computer programme. Guidelines for construction of equilibrium elements which can be incorporated in any standard computer programme were published in a paper by Watwood and Harz[14]. The difficulty in employing the method in shell analysis lies in the requirement of exact *a priori* satisfaction of field and boundary equilibrium. The idea of overcoming this obstacle is of the authors. It has been demonstrated on the simple case of curved bars[15, 16]. A clear physical reasoning can be summarized in the following sequence of statements:

(a) The pure equilibrium method converges in compatibility with refinement of finite element mesh.

(b) Exact equilibrium satisfaction is abandoned in the present approach but it is satisfied at least to the same order of accuracy as compatibility.

(c) Exact overall equilibrium is assumed to be satisfied in each element and along each particular boundary.

(d) The residual loading obtained after substitution of numerical results into the exact governing equations is self-equilibrating. It is of a local nature and vanishes with decreasing element size.

(e) Convergence in equilibrium is at least as fast as that of compatibility. The solution for any particular subdivision can be seen as an exact equilibrium result for a slightly different loading. The difference in loading is described in paragraph (d).

(f) Finally satisfaction of exact overall equilibrium can also be relaxed. The residual unbalanced loading should be of smaller order than the residual self-equilibrating one.

Paragraphs (a)–(f) outline the physical basis upon which the proposed shell element is constructed. Naghdi's[17, 18] shell equilibrium equations and complementary energy expression are employed. A very favourable property of the equilibrium shell element is its versatility with respect to the shell thickness. No artificial manipulation is necessary to handle thick or thin shell situations. Shell structures of arbitrary shape and loading can be treated as well. All the shell boundary variables have a parabolic distribution. On the assembly level the degrees of freedom at each side "node" consist of three displacement and two out of plane rotation components. The whole element thus has 45 degrees of freedom. Quadratic convergence both in stresses and displacements can be considered to be the most important characteristic of the new element. It can be incorporated in standard computer analysis systems. Furthermore a complete library of flat plate elements, three dimensional elements etc. can be consistently developed. In comparison with other high precision shell elements, the proposed one possesses certain advantageous features for which an extra amount of computational effort on the elemental level has to be paid.

A STRESS MODEL APPLICABLE WHEN EXACT *A PRIORI* EQUILIBRIUM SATISFACTION IS IMPOSSIBLE

The variational principle upon which the proposed shell finite element is outlined respresents a further modification of a generalized Hellinger–Reissner principle attributed to Washizu[19]. Due to the general nature of the idea and desire for a clear interrelation picture with other principles, the functional is first presented in its three dimensional linear elasticity form. Application to the shell equations is then straightforward and will be made in the next section. We adopt the notation in Appendix I of Ref. [19] with a few exceptions concerning the new extension. Accordingly the following symbolism is introduced using Cartesian tensor notation ($i, j, k, l = 1, 2, 3$):

σ_{ij} stress tensor
b_{ijkl} elastic compliance tensor
ϵ_{ij} strain tensor
$u_i, \tilde{u}_i$ displacement vector
T_i boundary traction vector

V volume (of an element)
S boundary of V
S_σ portion of S where traction is prescribed
S_u portion of S where displacements are prescribed
n_i direction cosines of normal directed outwards to S
$\bar{f}_i$ prescribed body force vector
$\bar{T}_i$ prescribed boundary traction vector (on S_σ)
$\bar{u}_i$ prescribed displacement vector (on S_u).

The functional is a special version of a perturbed complementary energy expression:

$$\pi_{mc}^* = \sum \left\{ \int_V [\tfrac{1}{2} b_{ijkl}\sigma_{ij}\sigma_{kl} + (\sigma_{ij,j} + \bar{f}_i)u_i] \, dV \right.$$
$$\left. - \int_S T_i(\tilde{u}_i^{(1)} + \tilde{u}_i^{(2)}) \, dS + \int_{S_\sigma} \bar{T}_i(\tilde{u}_i^{(1)} + \tilde{u}_i^{(2)}) \, dS \right\} \tag{1}$$

with σ_{ij}, u_i, $\tilde{u}_i^{(1)}$ and $\tilde{u}_i^{(2)}$ being the independent quantities subject to variation. The displacement vectors $\tilde{u}_i^{(1)}$ and $\tilde{u}_i^{(2)}$ are defined on the elemental boundaries only. $\tilde{u}_i^{(1)}$ is specified common for two neighbouring elements while σ_{ij}, u_i and $\tilde{u}_i^{(2)}$ are specific for each single element and as such can be eliminated on the elemental level of analysis. The assembly level of analysis is thus performed purely on values of $\tilde{u}_i^{(1)}$ and the subsidiary condition:

$$\tilde{u}_i^{(1)} = \bar{u}_i \quad \text{on } S_u \tag{2}$$

is easily enforced as in the familiar displacement model. S_u associated with $\tilde{u}_i^{(2)}$ is assumed to be nonexistent. Further $\tilde{u}_2^{(2)}$ is chosen orthogonal to $T_i^{(1)}$ and $\bar{T}_i^{(1)}$ defining the partitions $T_i = T_i^{(1)} + T_i^{(2)}$ and $\bar{T}_i = \bar{T}_i^{(1)} + \bar{T}_i^{(2)}$. This allows suppression of traction modes, of which continuity is undesired, independently for all the elements joining a common boundary.

Taking into account the relations

$$T_i = \sigma_{ij} n_j \quad \text{on } S \tag{3}$$

and

$$\epsilon_{ij} = \tfrac{1}{2}(u_{i,j} + u_{j,i}) \quad \text{in } V \tag{4}$$

the stationary conditions for π_{mc}^* obtained by the requirement

$$\delta\pi_{mc}^* = 0 \tag{5}$$

appear as:

$$\left.\begin{aligned} b_{ijkl}\sigma_{kl} - \epsilon_{ij} &= 0 \\ \sigma_{ij,j} + \bar{f}_i &= 0 \end{aligned}\right\} \quad \text{in } V \tag{6, 7}$$

$$u_i - \tilde{u}_i^{(1)} - \tilde{u}_i^{(2)} = 0 \quad \text{on } S \tag{8}$$

$$\left.\begin{aligned} T_i^{(2)} - \bar{T}_i^{(2)} &= 0 \\ \Sigma(T_i^{(1)} - \bar{T}_i^{(1)}) &= 0 \end{aligned}\right\} \quad \text{on } S_\sigma. \tag{9, 10}$$

When tractions are prescribed on an interelement boundary their intensity is given by $\Sigma\bar{T}_i$. Their distribution among the elements involved is arbitrary. Obviously the equilibrium condition $\Sigma(T_i - \bar{T}_i) = 0$ always holds.

The following goals have guided the authors towards construction of the functional π_{mc}^*:

(a) Stresses (forces) as well as displacements should be obtainable as primary result of analysis and with the same order of accuracy.

(b) Boundary traction representation should be consistent with the order of accuracy to which the stress approximation is capable of reproducing the true solution. Simultaneously the internal and boundary displacement fields u_i and $\tilde{u}_i^{(1)}$ should be represented consistently. The capability of u_i to match $\tilde{u}_i^{(1)}$ on the boundary is of special importance when extension to dynamic problems is considered.

(c) The various expressions involved in $\Delta\pi_{mc}^*$ = the difference in π_{mc}^*, between the exact and Ritz solutions, should allow the same convergence rate (provided convergence exists). If this is achieved as close as possible convergence is optimal.

Paragraph (c) invites a further observation. Let the superscripts E and R relate to the exact and Ritz solutions respectively. It is not difficult to show that the difference in π_{mc}^* is given by:

$$\Delta\pi_{mc}^* = \pi_{mc}^{*E} - \pi_{mc}^{*R} = \sum \left\{ \int_V [\tfrac{1}{2} b_{ijkl}(\sigma_{ij}^E - \sigma_{ij}^R)(\sigma_{kl}^E - \sigma_{kl}^R) + (\sigma_{ij,j}^E - \sigma_{ij,j}^R)(u_i^E - u_i^R)] \, dV - \int_S (T_i^E - T_i^R)(u_i^E - \tilde{u}_i^{(1)R} - \tilde{u}_i^{(2)R}) \, dS \right\}. \tag{11}$$

The first expression (the only one in the pure equilibrium method) represents the difference in complementary energy. Difference in equilibrium is given by the second and third expressions in V and on S respectively. We assume the approximate quantities σ_{ij}^R, u_i^R and $\tilde{u}_i^{(1)R}$ can reproduce the true solution up to the highest order of complete polynomial p incorporated in their shape functions. p is chosen common to all the quantities mentioned and obviously determines also the extent to which the actual boundary traction can be reproduced by $T_i^{(1)R}$. Let h denote a measure of maximum diameter representing the elemental size. Accordingly the first expression has the order h^{2p+2}. Inclusion of incomplete polynomial terms of order $p+1$ in σ_{ij} allows improvements in internal equilibrium satisfaction. The second expression then reaches as well the order h^{2p+2}. In both expressions the power $2p+2$ is not influenced by finite element mesh refinement since summation and integration is carried out over a constant total volume. This is not the case for the line integral expression. The total boundary length increases with systematic mesh refinement by the rate of h^{-1}. $T_i^{(2)}$ and $\tilde{u}_i^{(2)}$ are designed as to consist of polynomial terms of order $p+1$. Observing eqns (8) and (9) it turns out that the first and second terms in the line integral have the orders h^{p+1} and h^{p+2} respectively. The total order of the boundary expression is finally also h^{2p+2}.

The pure equilibrium method allows true stress reproduction up to order p, while equilibrium in $V+S$ is exactly satisfied by the Ritz solution. The key idea of the present approach lies in finding a technique permitting systematic satisfaction of equilibrium in $V+S$ to a controllable extent. That extent, in the shell element derived, is determined by optimal convergence.

APPLICATION TO SHELLS

Through application to shells of the functional π_{mc}^* introduced in the previous section, we employ results from the theory of shells [17, 18] and the differential geometry of a surface without any recapitulation of material. We adopt as close as possible the notation of Ref. [17]. In the following list of symbols the various surface tensors are presented in component form. Greek indices span the range 1, 2:

a_{ij}	metric tensor
a	$\det \lvert a_{ij} \rvert$
$b_{\alpha\beta}, b_\beta^\alpha$	curvature tensors
ν_α	unit vector normal to boundary
λ_α	unit vector tangent to boundary
$N^{\alpha\beta}, N^{\alpha\beta}, N^\alpha$	membrane forces
$M^{\alpha\beta}, M^\alpha$	bending moments
Q^α, Q	shear forces
$b_{\alpha\beta\gamma\delta}, c_{\alpha\beta}$	elastic compliance tensors
$\bar{p}^\alpha, \bar{p}$	prescribed surface forces
$\bar{m}^\alpha$	prescribed surface couples

$\bar{N}^\alpha, \bar{M}^\alpha, \bar{Q}$ prescribed values of N^α, M^α, Q
$u_\alpha, \tilde{u}_\alpha, w, \tilde{w}$ displacements
$\beta_\alpha, \tilde{\beta}_\alpha$ rotations
A area (of element)
L, L_σ, L_u boundary of A
t thickness.

The relations required for construction of π^*_{mc} in a form convenient for numerical analysis are described in the following paragraphs (a) to (c).

(a) A complementary energy function W_c according to Ref. [18] (with $M^{3\alpha} = V^3 = 0$) can be expressed as:

$$W_c = \frac{1}{2t}\left[b_{\alpha\beta\gamma\delta}\left(N'^{\alpha\beta}N'^{\gamma\delta} + \frac{12}{t^2}M^{\alpha\beta}M^{\gamma\delta}\right) + \frac{6}{5}C_{\alpha\beta}Q^\alpha Q^\beta\right] \tag{12}$$

where the symmetric membrane force tensor is given by:

$$N'^{\alpha\beta} = N^{\alpha\beta} + b_\gamma{}^\beta M^{\gamma\alpha} \tag{13}$$

and the moment tensor $M^{\alpha\beta}$ is symmetric.

For an isotropic elastic material with E, G, ν being the Young modulus, shear modulus and Poisson's ratio respectively, we have:

$$b_{\alpha\beta\gamma\delta} = \frac{1}{E}[\nu a_{\alpha\beta}a_{\gamma\delta} - (1+\nu)a_{\alpha\delta}a_{\beta\gamma}] \tag{14}$$

$$C_{\alpha\beta} = \frac{1}{G}a_{\alpha\beta}. \tag{15}$$

(b) Field equilibrium equations take the well known classical form:

$$N^{\beta\alpha}_{|\beta} - b_\gamma{}^\alpha Q^\gamma + \bar{p}^\alpha = 0 \tag{16}$$

$$Q^\alpha_{|\alpha} + t_{\alpha\gamma}N^{\gamma\alpha} + \bar{p} = 0 \tag{17}$$

$$M^{\beta\alpha}_{|\beta} - Q^\alpha + \bar{m}^\alpha = 0 \tag{18}$$

$$\bar{\epsilon}_{\alpha\beta}(N^{\beta\alpha} - b_\gamma{}^\beta M^{\gamma\alpha}) = 0 \tag{19}$$

where the $\bar{\epsilon}$-system for the surface is defined by:

$$\bar{\epsilon}_{11} = \bar{\epsilon}_{22} = 0; \qquad \bar{\epsilon}_{12} = -\bar{\epsilon}_{21} = a^{1/2}.$$

Equation (19) is homogeneous due to assuming the absence of in plane couples and will be satisfied exactly by the finite element approximation.

(c) Boundary equilibrium equations are conveniently transformed to a new orthogonal coordinate system created on the boundaries by the triplet of unit vectors according to Fig. 1.

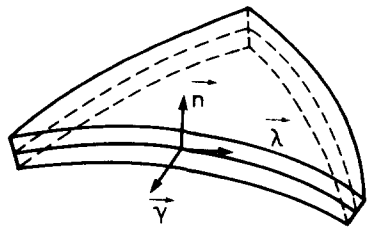

Fig. 1.

In that system all the tensors involved are represented directly by their physical components. Results provided by the program are extremely easy for interpretation by the user. This natural global coordinate system is inherent in the proposed finite element model comprising only side nodes.

The resulting equations are:

$$\Sigma(N^{\alpha(1)} - \bar{N}^{\alpha(1)}) = 0; \tag{20}_1$$

$$N^{\alpha(2)} - \bar{N}^{\alpha(2)} = 0 \tag{20}_2$$

$$\Sigma(M^{\alpha(1)} - \bar{M}^{\alpha(1)}) = 0; \tag{21}_1$$

$$M^{\alpha(2)} - \bar{M}^{\alpha(2)} = 0 \tag{21}_2$$

$$\Sigma(Q^{(1)} - \bar{Q}^{(1)}) = 0; \tag{22}_1$$

$$Q^{(2)} - \bar{Q}^{(2)} = 0 \tag{22}_2$$

where the boundary forces are obtained as a partial product of a standard tensorial transformation from one coordinate system to another:

$$N^1 = N^{\alpha\beta}\nu_\alpha\nu_\beta \tag{23}$$

$$N^2 = N^{\alpha\beta}\nu_\alpha\lambda_\beta \tag{24}$$

$$M^1 = M^{\alpha\beta}\nu_\alpha\nu_\beta \tag{25}$$

$$M^2 = M^{\alpha\beta}\nu_\alpha\lambda_\beta \tag{26}$$

$$Q = Q^\alpha\nu_\alpha. \tag{27}$$

Boundary displacements $\tilde{u}_\alpha$, $\tilde{w}$ and $\tilde{\beta}_\alpha$ appearing in the line integral products are defined consistently in the new coordinate system.

By means of eqns (12), (16–18), (20–22) the functional π^*_{mc} takes its particular form when applied to shells:

$$\pi^*_{mc} = \sum \left\{ \int_A [W_c + (N^{\beta\alpha}_{|\beta} - b_\gamma{}^\alpha Q^\gamma + \bar{p}^\alpha)u_\alpha + (Q^\alpha_{|\alpha} + b_{\alpha\gamma}N^{\gamma\alpha} + \bar{p})w + (M^{\beta\alpha}_{|\beta} - Q^\alpha + \bar{m}^\alpha)\beta_\alpha]\,dA \right.$$
$$- \int_L [N^\alpha(\tilde{u}_\alpha{}^{(1)} + \tilde{u}_\alpha{}^{(2)}) + M^\alpha(\tilde{\beta}_\alpha{}^{(1)} + \tilde{\beta}_\alpha{}^{(2)}) + Q(\tilde{w}^{(1)} + \tilde{w}^{(2)})]\,dL + \int_{L_u} [\bar{N}^\alpha(\tilde{u}_\alpha{}^{(1)} + \tilde{u}_\alpha{}^{(2)})$$
$$\left. + \bar{M}^\alpha(\tilde{\beta}_\alpha{}^{(1)} + \tilde{\beta}_\alpha{}^{(2)}) + \bar{Q}(\tilde{w}^{(1)} + \tilde{w}^{(2)})]\,dL \right\}. \tag{28}$$

Equations (16)–(18), (20)–(22) are obviously obtained as stationary conditions for π^*_{mc}. In addition the vanishing of $\delta\pi^*_{mc}$ supplies the stress-displacement relations:

$$\frac{1}{t} b_{\alpha\beta\gamma\delta}N'^{\gamma\delta} - \frac{1}{2}(u_{\alpha|\beta} + u_{\beta|\alpha}) + b_{\alpha\beta}w = 0 \tag{29}$$

$$\frac{12}{t^3} b_{\alpha\beta\gamma\delta}M^{\gamma\delta} - \frac{1}{2}[\beta_{\alpha|\beta} + \beta_{\beta|\alpha} - b_\alpha{}^\gamma(u_{\gamma|\beta} - b_{\gamma\beta}w) - b_\beta{}^\gamma(u_{\gamma|\alpha} - b_{\gamma\alpha}w] = 0 \tag{30}$$

$$\frac{6}{5t} C_{\alpha\beta}Q^\beta - \beta_\alpha - w_{,\alpha} - b_\alpha{}^\gamma u_\gamma = 0 \tag{31}$$

provided the subsidiary conditions on L_u:

$$\tilde{u}_\alpha{}^{(1)} = \bar{u}_\alpha \tag{32}$$

$$\tilde{w}^{(1)} = \bar{w} \tag{33}$$

and

$$\tilde{\beta}_\alpha^{(1)} = \tilde{\beta}_\alpha \tag{34}$$

are fulfilled.

DISCRETIZATION TECHNIQUE

In this section discretization of the governing equations and shell geometry is dealt with in general. For more detailed information concerning the technique employed the interested reader is advised to consult Ref. [28].

The element is defined by the choice of a group of 28 points located on the shell middle surface according to Fig. 2. Three points at each side, for instance 1–4–2, 2–5–3, 3–6–1, serve as elemental nodes.

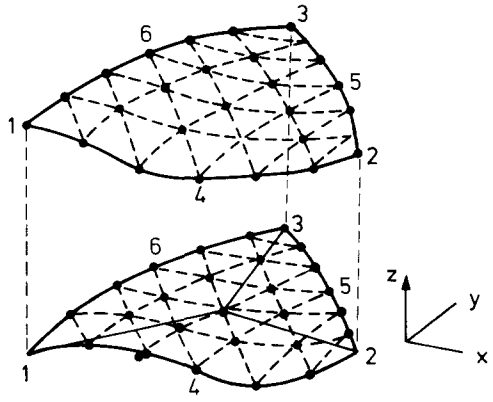

Fig. 2.

A cartesian coordinate system is fixed in the plane passing through the three element corner points defining a curvilinear coordinate system on the shell surface (see Fig. 2). The 28 points chosen allow a 6th order polynomial representation of the middle surface as well as its boundaries projected onto the reference plane. It is worth mentioning that boundaries common to two elements will take different shapes when projected onto the different reference planes. This assures that integration over the projected areas covers the whole shell surface involved without creating any gaps or overlaps.

The approximation of geometry introduced yields an error of order h^4 in $b^\alpha_{\beta,\gamma}$. This is one order better than the minimum necessary for not spoiling equilibrium accuracy by insufficient approximation of the geometry.

Let the column vectors $\boldsymbol{\sigma}$, $\mathbf{v}$ and $\mathbf{v}^{(k)}$ $(k = 1, 2)$ denote consistent sequential arrangement of components of the force, internal and boundary displacement tensors. Then following the standard finite element technique we can write:

$$\boldsymbol{\sigma} = \mathbf{P}\boldsymbol{\beta} \tag{35}$$

$$\mathbf{v} = \mathbf{L}\boldsymbol{\alpha} \tag{36}$$

$$\mathbf{v}^{(k)} = \mathbf{L}^{(k)}\boldsymbol{\alpha}^{(k)}; \quad k = 1, 2 \tag{37}$$

where $\mathbf{P}$, $\mathbf{L}$ and $\mathbf{L}^{(k)}$ are shape function matrices and $\boldsymbol{\beta}$, $\boldsymbol{\alpha}$ and $\boldsymbol{\alpha}^{(k)}$ are the unknown Ritz coefficient column vectors. The structure of $\mathbf{P}$, $\mathbf{L}$ and $\mathbf{L}^{(k)}$ must be illuminated further. $\mathbf{P}$ comprises complete second order polynomials for every component $N'^{\alpha\beta}$ and Q^α as well as complete third order polynomials for each component $M^{\alpha\beta}$. In addition incomplete 3rd and 4th order polynomials are included allowing satisfaction of internal force and rotational equilibrium up to orders 2 and 3 respectively. This yields representation of boundary forces to order 3 while boundary moment components are represented up to order 4. Arrangement of these in column

vector form $\mathbf{T}$ gives:

$$\mathbf{T} = \mathbf{P}_b \boldsymbol{\beta} \tag{38}$$

where $\mathbf{P}_b$ is a boundary shape function matrix. w as well as the components u_α are represented by complete second order polynomials in $\mathbf{L}$ while the rotation components β_α by complete third order ones.

Each boundary displacement and rotation component has a complete 2nd order polynomial representation in $\mathbf{L}^{(1)}$.

The matrix $\mathbf{L}^{(2)}$ consists of Legendre polynomials. Their order for displacement components is 3 while those belonging to moment components have the orders 3 and 4.

In fact the field force and displacement variables are defined independently in each of the three subelements according to Fig. 2. The force quantities are interrelated by means of exact intersubelement equilibrium satisfaction. The argument for employing that sort of technique is explained in Ref. [14] and will not be repeated here. It is assumed that $\boldsymbol{\sigma}$ and $\mathbf{v}$ comprise the total number of independent quantities as well as that the $\int$ sign symbolizes integration over all the three subregions. It remains yet to cast the elastic compliance tensor components into a matrix form $\mathbf{C}$ and the components of body force and surface force tensors into vector form $\bar{\boldsymbol{\sigma}}$ and $\bar{\mathbf{T}}$ respectively. Doing so we are able to express field equilibrium in matrix notation

$$\mathbf{B}\boldsymbol{\sigma} + \bar{\boldsymbol{\sigma}} = 0 \tag{39}$$

where $\mathbf{B}$ is a differential operator matrix.

Finally eqns (35)–(39) allow expression of π^*_{mc} in matrix form:

$$\pi^*_{mc} = \Sigma[\tfrac{1}{2}\boldsymbol{\beta}^T\mathbf{H}\boldsymbol{\beta} + \boldsymbol{\alpha}^T(\mathbf{M}\boldsymbol{\beta} + \mathbf{N}) - \boldsymbol{\alpha}^{(1)T}(\mathbf{G}^T\boldsymbol{\beta} - \mathbf{T}^{(1)}) - \boldsymbol{\alpha}^{(2)T}(\mathbf{F}^T\boldsymbol{\beta} - \mathbf{T}^{(2)})] \tag{40}$$

with

$$\mathbf{H} = \int_A \mathbf{P}^T\mathbf{C}\mathbf{P}\,\mathrm{d}A \tag{41}$$

$$\mathbf{M} = \int_A \mathbf{L}^T\mathbf{B}\mathbf{P}\,\mathrm{d}A \tag{42}$$

$$\mathbf{N} = \int_A \mathbf{L}^T\bar{\boldsymbol{\sigma}}\,\mathrm{d}A \tag{43}$$

$$\mathbf{G} = \int_L \mathbf{P}_b{}^T\mathbf{L}^{(1)}\,\mathrm{d}L \tag{44}$$

$$\mathbf{F} = \int_L \mathbf{P}_b{}^T\mathbf{L}^{(2)}\,\mathrm{d}L \tag{45}$$

$$\mathbf{T}^{(1)} = \int_L \mathbf{L}^{(2)}\bar{\mathbf{T}}\,\mathrm{d}L \tag{46}$$

$$\mathbf{T}^{(2)} = \int_L \mathbf{L}^{(2)}\bar{\mathbf{T}}\,\mathrm{d}L. \tag{47}$$

We first utilize the fact that a part of the Ritz coefficients is specific for each element. The stationary condition for π^*_{mc} with respect to variation of $\boldsymbol{\alpha}$ and $\boldsymbol{\alpha}^{(2)}$ is:

$$\frac{\partial\pi^*_{mc}}{\partial\boldsymbol{\alpha}} = \mathbf{M}\boldsymbol{\beta} + \mathbf{N} = \mathbf{0} \tag{48}$$

$$\frac{\partial\pi^*_{mc}}{\partial\boldsymbol{\alpha}^{(2)}} = -\mathbf{F}^T\boldsymbol{\beta} + \mathbf{T}^{(2)} = \mathbf{0} \tag{49}$$

or

$$\mathbf{A}\boldsymbol{\beta} + \mathbf{R} = \mathbf{0} \tag{50}$$

where

$$\mathbf{A} = \left| \frac{\mathbf{M}}{-\mathbf{F}^T} \right| \tag{51}$$

and

$$\mathbf{R} = \left\{ \frac{\mathbf{N}}{\mathbf{T}^{(2)}} \right\}. \tag{52}$$

Equations (48) approximates field equilibrium in an element. Due to orthogonality of Legendre polynomials to every polynomial of lower order than their own eqn (49) assures approximate satisfaction of boundary equilibrium independently for each element for boundary traction modes of higher order than 2. Thus only traction modes up to order 2 are left to be continuous keeping the order of reproduction of true forces equal inside the element and along its boundaries. Without loss of generality we can assume the convenient arrangement of $\mathbf{A}$ and $\boldsymbol{\beta}$:

$$\mathbf{A} = |\bar{\mathbf{A}}|\bar{\bar{\mathbf{A}}}| \tag{53}$$

$$\boldsymbol{\beta} = \left\{ \frac{\bar{\boldsymbol{\beta}}}{\bar{\bar{\boldsymbol{\beta}}}} \right\} \tag{54}$$

where $\bar{\bar{\mathbf{A}}}$ is positive definite and $\bar{\bar{\boldsymbol{\beta}}}$ is to be eliminated:

$$\bar{\bar{\boldsymbol{\beta}}} = -\bar{\bar{\mathbf{A}}}^{-1}(\bar{\mathbf{A}}\bar{\boldsymbol{\beta}} + \mathbf{R}). \tag{55}$$

We get:

$$\boldsymbol{\beta} = \mathbf{D}^T\bar{\boldsymbol{\beta}} - \bar{\mathbf{R}} \tag{56}$$

by means of:

$$\mathbf{D}^T = \left| \frac{\mathbf{I}}{-\bar{\bar{\mathbf{A}}}^{-1}\bar{\mathbf{A}}} \right| \tag{57}$$

and

$$\bar{\mathbf{R}} = \left\{ \frac{\mathbf{0}}{\bar{\bar{\mathbf{A}}}^{-1}\mathbf{R}} \right\}. \tag{58}$$

If desired the values of $\boldsymbol{\alpha}$ can be calculated from an appropriate part of the equations $(\partial\pi^*_{mc})/(\partial\boldsymbol{\beta})$.

Employing eqn (56) in eqn (40) a new form of π^*_{mc} is obtained:

$$\bar{\pi}^*_{mc} = \Sigma[\tfrac{1}{2}\bar{\boldsymbol{\beta}}^T\bar{\mathbf{H}}\bar{\boldsymbol{\beta}} - \mathbf{Z}^T\bar{\boldsymbol{\beta}} - \boldsymbol{\alpha}^{(1)T}(\bar{\mathbf{G}}^T\bar{\boldsymbol{\beta}} - \bar{\mathbf{T}}^{(1)})] + C_1 \tag{59}$$

where $$C_1 = \tfrac{1}{2}\Sigma\bar{\mathbf{R}}^T\mathbf{H}\bar{\mathbf{R}}$$

and $$\bar{\mathbf{H}} = \mathbf{D}\mathbf{H}\mathbf{D}^T \tag{60}$$

$$\bar{\mathbf{G}} = \mathbf{D}\mathbf{G} \tag{61}$$

$$\bar{\mathbf{T}}^{(1)} = \mathbf{G}^T\bar{\mathbf{R}} + \mathbf{T}^{(1)} \tag{62}$$

$$\mathbf{Z} = \mathbf{DH}\bar{\mathbf{R}}. \tag{63}$$

The stationary condition of $\bar{\pi}^*_{mc}$ with respect to variation of $\bar{\boldsymbol{\beta}}$ is:

$$\frac{\partial \pi^*_{mc}}{\partial \bar{\boldsymbol{\beta}}} = \bar{\mathbf{H}}\bar{\boldsymbol{\beta}} - \mathbf{Z} - \bar{\mathbf{G}}\boldsymbol{\alpha}^{(1)} = \mathbf{0}. \tag{64}$$

$\bar{\mathbf{H}}$ is symmetric and positive definite hence $\bar{\boldsymbol{\beta}}$ can be calculated as:

$$\bar{\boldsymbol{\beta}} = \bar{\mathbf{H}}^{-1}(\bar{\mathbf{G}}\boldsymbol{\alpha}^{(1)} + \mathbf{Z}). \tag{65}$$

Substitution for $\bar{\boldsymbol{\beta}}$ into eqn (59) finally provides the familiar functional:

$$\pi = \Sigma[\tfrac{1}{2}\boldsymbol{\alpha}^{(1)T}\mathbf{K}\boldsymbol{\alpha}^{(1)} - \boldsymbol{\alpha}^{(1)T}\bar{\mathbf{S}}] + C_2 \tag{66}$$

with the element stiffness matrix

$$\mathbf{K} = \bar{\mathbf{G}}^T\bar{\mathbf{H}}^{-1}\bar{\mathbf{G}} \tag{67}$$

and the element loading vector

$$\bar{\mathbf{S}} = \bar{\mathbf{T}}^{(1)} - \bar{\mathbf{G}}^T\bar{\mathbf{H}}^{-1}\mathbf{Z}, \tag{68}$$

The constant $C_2 = \frac{1}{2}\Sigma\mathbf{Z}^T\bar{\mathbf{H}}^{-1}\mathbf{Z} - C_1$ has no influence on the results. The process of assembling the element matrices into global ones is the same as in the displacement model and will not be repeated here. After $\boldsymbol{\alpha}^{(1)}$ is evaluated the coefficients $\boldsymbol{\beta}$ can be calculated from eqns (65) and (55).

NOTES ON CONVERGENCE OF THE ELEMENT

When an exact solution is to be reached as the limit of a sequence of approximate solutions completeness consideration demands determination of the space of all the solution functions. The following most singular forms of loadings, geometric and material properties are assumed to appear in the shell domain: point loads, piecewise continuous surface couples, shell thickness, elastic compliance and curvature tensor components. The space of permissible force, moment and displacement tensor components then can be found by inspection of π^*_{mc} term by term. π^*_{mc} remains uniquely defined if the degree of component singularity does not exceed the following limits:

$N^{\alpha\beta}, Q^{\alpha}, \beta_{\alpha}$—piecewise continuous;

$M^{\alpha\beta}, u_{\alpha}, w$—continuous.

In order to exploit the full element capability of the true solution reproduction we enforce a continuity restriction which always can be easily obeyed by judicious lying down of finite element mesh. We require the loadings and other shell data to fulfill in every element the smoothness conditions: Prescribed forces, shell thickness and elastic compliance constants having continuous second derivatives. Prescribed couples and shell curvature components having continuous third derivatives. Discontinuities in lower order derivatives are assumed to occur on the element boundaries and corners.

With those restrictions satisfied a proof of convergence with a rate of h^3 of all the quantities involved has been found by the authors in the spirit of Refs [16] and [27]. It turned out, however, that a general way for convergence investigation of a broad class of mixed and hybrid models has been recently worked out by Oden and his co-workers† (partly in print at the time

†The authors are indebted to Prof. J. T. Oden for his kindly supplying of the most updated material.

the present paper is being written). It is believed by the authors that application of the general theory contained in the series of Refs [20]–[24] to a particular case of the proposed shell model can be made. It is undoubtedly a lengthy procedure lying outside the scope of the present paper.

NUMERICAL STUDIES

It is expected that an exhaustive series of numerical examples will not only verify the proven rate of convergence but also yield recommendations for mesh size selection in typical cases of shell behavior. The two extreme situations when pure bending or membrane action results as a solution of the coupled shell equations are revealing.

(a) The pure bending situation. Let $\bar{M}$ denote a prescribed boundary moment causing pure bending and l a typical wavelength. (For clarification of the concept of wave length in shells see Ref. [25].) Then equality in complementary energy error ($o(h^3)$) implies the following relation for the residual membrane forces (component indices omitted) provided the shell is isotropic:

$$N^R = N^R - N^E = \frac{1}{t} o(M^R - M^E) = \frac{\bar{M}}{l}\frac{l}{t} o\left(\frac{h}{l}\right)^3. \tag{69}$$

Only when $h^3/l^2 t \leq o(1)$ can we expect N^R to begin to vanish relative to $\bar{M}/l$. This enforces a choice of elemental size of

$$h \leq o(\sqrt[3]{tl^2}). \tag{70}$$

It turns out that the case treated is the most unfavourable one, due to the special structure of the proposed finite element model. An assessment of elemental size needed in such a situation will be made for the case of a slit cylinder in pure torsion. The geometry of the panel analyzed is essentially the same as in Ref. [8]. It is approximated by joining two triangular elements according to Fig. 3. Since in this case $l = R$, eqn (70) yields:

$$h \leq o(\sqrt[3]{10}) \quad \text{or} \quad \varphi \leq o(0.2).$$

Table 1 contains results for twist per unit length (θ), twisting moment ($M \times \varphi$) and order of membrane forces for various values of φ. The results appearing in Ref. [8] are compared with those obtained by use of the proposed element. In Ref. [8] the rigid body modes are secured in two different ways: (1) $w = u_1 = u_2 = 0$ at one corner, $w = u_1 = 0$ at another corner and $w = 0$ at a third corner. (2) $w = 0$ at all the four corners and $u_1 = u_2 = 0$ at one corner.

The elements tested in Ref. [8] appear to be sensitive with respect to the manner of securing rigid body modes. No significant differences have been obtained with the proposed element for various alternatives of boundary conditions which avoid rigid body motion. This insensitivity can be seen as an inherent feature of the new shell element.

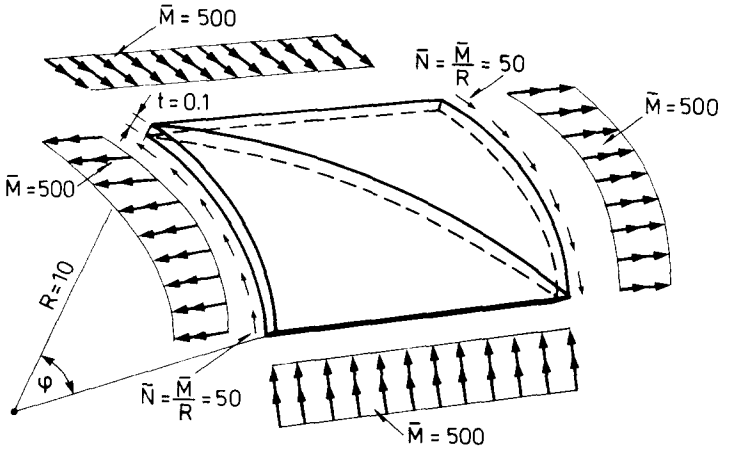

Fig. 3.

Table 1.

		$\theta \times 10^5$	$M_{x\varphi} = M^{12} = M^{21}$	$o(N^{\alpha\beta})$
	$\varphi = 0.01$			
Ref. [8]	24 d.o.f., b.c.1	7.77	496	$o[5]$
	24 d.o.f., b.c.2	7.80	497	$o[0.1]$
	48 d.o.f., b.c.2	7.80	499	$o[0.1]$
	Sheba 3	7.80	500	$o[0.1]$
	Present approach	7.80	500	$o[0.0002]$
	Classical	7.80	500	$o[5]$
	$\varphi = 0.1$			
		$\theta \times 10^5$	$M_{x\varphi} = M^{12} = M^{21}$	$o(N^{\alpha\beta})$
Ref. [8]	24 d.o.f., b.c.1	7.16	460	$o[M_{x\varphi}]$
	24 d.o.f., b.c.2	7.80	497	$o[0.1]$
	48 d.o.f., b.c.1	7.77	498	$o[0.1]$
	48 d.o.f., b.c.2	7.80	499	$o[0.1]$
	Sheba 3	7.80	500	$o[4]$
	Present approach	7.80	500	$o[2]$
	Classical	7.80	500	$o[5]$
	$\varphi = 0.2$			
		$\theta \times 10^5$	$M_{x\varphi} = M^{12} = M^{21}$	$o(N^{\alpha\beta})$
Ref. [8]	24 d.o.f., b.c.1	5.57	448	$o[M_{x\varphi}]$
	48 d.o.f., b.c.1	7.74	496	$o[5]$
	Present approach	7.80	500	$o[30]$
	Classical	7.80	500	$o[5]$

(b) Pure membrane action. Let $\bar{p}$ denote a prescribed loading and l again a typical wavelength. Analogous considerations to those of case "a" yield:

$$M^R = M^R - M^E = to(N^R - N^E) = \bar{p}l^2 \frac{t}{l} o\left(\frac{h}{l}\right)^3. \tag{71}$$

Hence M^R will have a vanishing tendency relative to $\bar{p}l^2$ when $th^3/l^4 \leq o(1)$, allowing a convenient choice of order for h:

$$h \leq o(l\sqrt[3]{l/t}). \tag{72}$$

Equation (72) states that in cases with l having the magnitude of shell span, a single element should suffice.

This will be demonstrated by analyzing a large cylindrical panel under membrane action (see Fig. 4). Two loading cases are considered, according to Fig. 5. The results are collected in Table 2 and compared with exact values. The results clearly verify the validity of eqn (72).

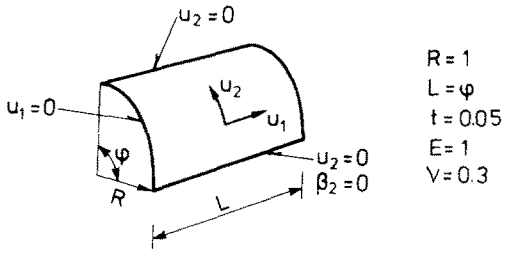

Fig. 4.

R = 1
L = φ
t = 0.05
E = 1
ν = 0.3

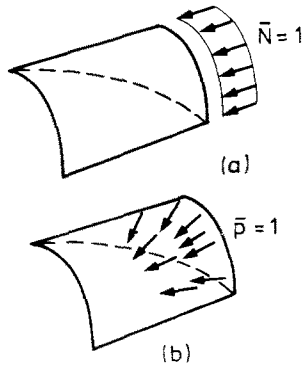

Fig. 5.

Table 2.

	Loading case 5a				Loading case 5b			
	u_1/L	N^{11}	$N^{\alpha\beta} \neq N^{11}$	$M^{\alpha\beta}$	u_1/L	N^{22}	$N^{\alpha\beta} \neq N^{22}$	$M^{\alpha\beta}$
$\varphi = 90°$	−19.6	−1.00	$o(10^{-4})$	$o(10^{-5})$	5.90	−1.01/−0.95	$o(5 \cdot 10^{-2})$	$o(10^{-3})$
$\varphi = 45°$	−19.97	−1.00	$o(10^{-5})$	$o(5 \cdot 10^{-7})$	5.993	−1.000	$o(5 \cdot 10^{-4})$	$o(10^{-5})$
exact	−20	−1.00	0	0	6	−1	0	0

(c) Shells subject to combined membrane and bending action. The example of a pinched sphere has been chosen to demonstrate the new shell element's ability to cope with the difficult case of rapid variation in shell behaviour. The same wedge of the shell has been analyzed as in Ref. [12] (see Fig. 6). In Table 3 results for normal deflection and membrane force under load and at the equator are presented together with the results of three other elements previously published in Ref. [12].

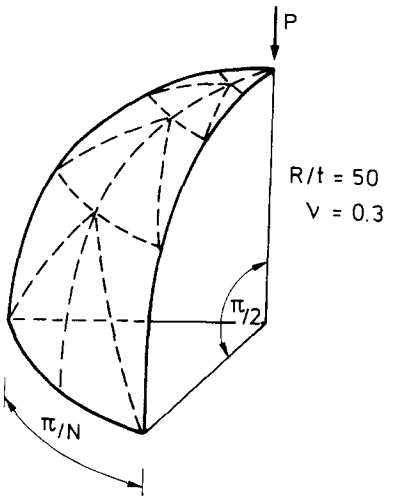

Fig. 6.

Table 3.

	Deflection under load $\lvert Etw^{(P)}/P\rvert$				Membrane force under load $\lvert RN^{11}_{(P)}/P\rvert = \lvert RN^{22}_{(P)}/P\rvert$			
N	CURSHL $(K-S)$	CURSHL $(D-V)$	*TSS*	Pres. element	CURSHL $(K-S)$	CURSHL $(D-V)$	*TSS*	Pres. element
2	12.79	12.73	18.10	24.76	1.65	1.68	7.05	11.11
4	20.67	20.57	20.95	23.60	7.85	8.00	8.64	11.89
6	21.08	20.98	21.11	22.36	9.34	9.56	9.76	10.83
	Koiter: 21.20							

	Deflection at equator $\lvert Etw^{(E)}/P\rvert$				Membrane force at equator $\lvert RN^{22}_{(E)}/P\rvert$			
N	CURSHL $(K-S)$	CURSHL $(D-V)$	*TSS*	Pres. element	CURSHL $(K-S)$	CURSHL $(D-V)$	*TSS*	Pres. element
2	0.2994	0.2993	0.0867	0.1857	0.0611	0.0615	0.3071	0.1591
4	0.2084	0.2083	0.2256	0.2069	0.1628	0.1627	0.1873	0.1592
6	0.2069	0.2072	0.2161	0.2069	0.1602	0.1602	0.1686	0.1592
	Membrane: 0.2069				Membrane: 0.1592			

(d) Moderately thick shells. One of the advantageous properties of the new element is its insensitivity with respect to the measure of thickness. In order to isolate the shear strain energy effect, a plate bending situation is considered, conveniently eliminating the effect of curvature. The case of a thick clamped circular plate under uniformly distributed load $\bar{p}$ is analyzed (see Fig. 7). Table 4 contains results for central deflection, moments and shear forces for the subdivisions $N = 1$ and $N = 2$. Comparison is made with exact solutions and with the relevant results of Ref. [10]. The results are in excellent agreement with theory even for a very coarse subdivision.

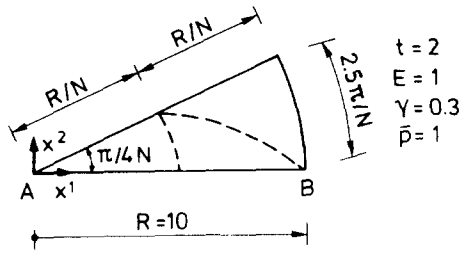

Fig. 7.

Table 4.

	$W^{(A)}$	$Q^1_{(A)}$	$Q^1_{(B)}$	$M^{11}_{(A)}$	$M^{11}_{(B)}$	$M^{22}_{(A)}$	$M^{22}_{(B)}$
$N = 1$, present approach	−270.50	0.000	5.00	−8.125	12.5	−8.125	3.75
$N = 2$, present approach	−253.37	0.002	4.99/5.01	−8.124/−8.146	12.5	−8.135	3.72/3.79
$N = 2$, Ref. [10]	−253.71	—	—	—	—	—	—
exact, ref. [26], shear. coef. $= \frac{3}{2}$	−262.03	0.000	5.00	−8.125	12.5	−8.125	3.75
exact, but shear. coef. $= \frac{6}{5}$	−252.28	0.000	5.00	−8.125	12.5	−8.125	3.75

CONCLUSIONS AND FUTURE CONSIDERATION

The theory of a new high-precision stress shell finite element is presented. It is tested on a broad class of shell problems which virtually cover the whole practical range. This versatility with respect to all kinds of shell situations is one of the favourable properties of the new element. Results obtained with the proposed element are in general not less accurate than those obtained by the known sophisticated elements. Equal accuracy of stresses and displacements is of both esthetic and practical importance. Having developed and tested the new element, the authors are presently seeking the most appropriate computer technique for working out estimates for practical utilization. This will hopefully be published in the near future.

REFERENCES

1. J. H. Argyris and D. W. Scharpf, The SHEBA family of shell elements for the matrix displacement method. *J. R. Aeronaut. Soc.* **72**, 873–883 (1968).
2. G. Dupuis, Application of Ritz's method to thin elastic shell analysis. *J. Appl. Mech.* **38**, 987–995 (1971).
3. G. R. Cowper, *CURSHL—a high-precision finite element for shells of arbitrary shape.* National Research Council of Canada Report (1972).
4. D. J. Dawe, High-order triangular finite element for shell analysis, *Int. J. Solids Structures* **11**, 1097–1110 (1975).
5. H. Fette, Gekrümmte finite Elemente zur Berechnung von Schalentragwerken; Schriftenreihe d. Inst. f. Konstr. Ingenieurbau d. Tech. Univ. Braunschweig, Heft 1, Werner-Vlg., Düsseldorf (1969).
6. B. E. Greene, R. E. Jones, R. W. McLay and D. R. Strome, Dynamic analysis of shells using doubly-curved finite elements, *Proc. 2nd Conf. on Matrix Meth. in Struct. Mech.* pp. 185–212. AFFDL Wright-Patterson AFB, Ohio (1969).
7. S. W. Key and Z. E. Beisinger, The analysis of thin shells by the finite element method, in: High speed computing of elastic structures. *Proc. of IUTAM Symposium, Liège* (Edited by B. Fraeijs de Veubeke), pp. 209–252 (1971).
8. A. J. Morris, A deficiency in current finite elements for thin shell applications. *Int. J. Solids Structures* **9**, 331–346 (1973).
9. W. Visser, The application of a curved mixed-type shell element, in: High speed computing of elastic structures. *Proc. of IUTAM Symposium, Liège* (Edited by B. Fraeijs de Veubeke), pp. 321–355 (1971).
10. O. C. Zienkiewicz, R. L. Taylor and J. M. Too, Reduced integration technique in general analysis of plates and shells. *Int. J. Num. Meth. Eng.* **3**, 275–290 (1971).
11. N. Lochner, Die Anwendung des Schalenelements SHEBA In: *Finite Elemente in der Statik* (Edited by E. Buck *et al.*), pp. 353–372. W. Ernst (1973).

12. G. R. Cowper, G. M. Lindberg and M. D. Olson, Comparison of two high-precision triangular finite elements for arbitrary deep shells. In *Proc. 3rd Conf. on Matrix Meth. in Struct. Mech.* pp. 227–304. AFFDL Wright-Patterson AFB, Ohio (1973).
13. B. Fraeijs de Veubeke, Displacement and equilibrium models in the finite element method. *Stress Analysis* (Edited by O. C. Zienkiewicz and G. S. Holister), chap. 9. Wiley, New York (1965).
14. V. B. Watwood and B. J. Harz, An equilibrium stress field model for finite element solutions of two-dimensional elastostatic problems. *Int. J. Solids Structures* **4**, 857–873 (1968).
15. M. Gellert, M. E. Laursen and M. P. Nielsen, Finite element equilibrium model for general body force distribution. *Bygningsstatiske Meddelelser*, **46**(1), 1–24 (1975).
16. M. Gellert and M. E. Laursen, Formulation and convergence of a mixed finite element method applied to elastic arches of arbitrary geometry and loading. *J. of Computer Meth. in Appl. Mech. and Eng.* **7**, 285–302 (1976).
17. P. M. Naghdi, Foundations of elastic shell theory. *Progress in Solid Mech.* (Edited by I. N. Sneddon and R. Hill), Vol. 4, pp. 1–90, North Holland, Amsterdam (1963).
18. P. M. Naghdi, The theory of plates and shells. *Encycl. of Physics* (Edited by S. Flügge), Vol. VIa/2, Mechanics of Solids II, pp. 425–640. Springer, Berlin (1972).
19. K. Washizu, *Variational Methods in Elasticity and Plasticity*, 2nd Edn, Pergamon, Oxford (1975).
20. J. T. Oden and J. N. Reddy, *An Introduction to the Mathematical Theory of Finite Elements*. Wiley, New York (1976).
21. J. T. Oden, Some contributions to the mathematical theory of mixed finite element approximations. *Tokyo Seminar on Finite Elements*, Univ. of Tokyo Printer (1973).
22. J. T. Oden and J. K. Lee, Theory of mixed and hybrid finite element approximations in linear elasticity. *IUTAM/IUM Symposium, Marseilles*, 1975 (to appear in Lecture Notes in Mathematics, Springer, Berlin).
23. J. N. Reddy and J. T. Oden, Mixed finite element approximations of linear boundary value problems. *Quart. of Appl. Math.* 255–280 (Oct. 1975).
24. J. T. Oden and J. N. Reddy, On mixed finite element approximations; *SIAM J. Num. Anal.* **13**, 393–404 (1976).
25. H. S. Rutten, *Theory and Design of Shells on the Basis of Asymptotic Analysis*. Rutten and Kruisman Consulting Engineers, Holland (1973).
26. S. Timoshenko, *Strength of Materials*, Part II, Advanced theory and problems, 3rd Edn. Van Nostrand, New York (1956).
27. C. Johnson, On the convergence of a mixed finite element method for plate problems. *Num. Math.* **21**, 43–62 (1972).
28. M. E. Laursen, *EQSHELL: An equilibrium finite element for arbitrary shell geometry*. Struct. Res. Lab., Techn. Univ. of Denmark, R77 (1977).